Energetics and Kinetics of Thermal Ionization Models of MALDI

Richard Knochenmuss
Tofwerk AG, Uttigenstr. 22
3600 Thun, Switzerland
rknochenmuss@gmx.net

Keywords: MALDI ionization, polar fluid model, thermal ionization

Abstract
Thermal models of ultraviolet MALDI ionization based on the polar fluid concept are rexamined. Key components are very high solvating power of the fluidized matrix and consequent low reaction free energy, attainment of thermal equilibrium in the fluid, and negligible recombination losses. None of these are found to hold in a MALDI event. The reaction free energy in the hot matrix must be near the gas phase value, ion formation is too slow to approach equilibrium, and geminate recombination of autoprotolysis pairs greatly increases the initial loss rate. The maximum thermal ion yield is estimated to be many orders of magnitude below experimental values.

Published in J. Am. Soc. Mass Spectrom.
http://dx.doi.org/10.1007/s13361-014-0931-y

Introduction

Models for MALDI ionization postulate widely varying roles for both the matrix and the laser. In the Lucky Survivors model, ions present in the preparation solution remain in the solidified sample and are merely liberated by the ablation process.[1-3] At the other end of the spectrum, the Coupled Chemical and Physical Dynamics (CPCD) model suggests that pooling reactions of electronic excited states leading to matrix primary ions are the main ionization pathway in ultraviolet MALDI.[4-7] In the middle are thermal models, in which matrix primary ions are formed due to laser heating of the sample. Electronic excitations are not necessary in these models, they are merely a means to convert laser energy to heat.

Thermal models of MALDI are not new.[8, 9] Most relevant here is the polar fluid model (PFM) which was proposed in qualitative form some time ago.[10, 11] It is based on the idea that, for a short time during ablation, the matrix is a dense, hot fluid, which facilitates ion pair separation by mechanisms similar to those in aqueous solutions. Examination of the fundamental energetics suggested ion yields would be far too low to be consistent with available data at the time the model was proposed.[12]

The PFM received little attention until recently, when MALDI ion yields were revisited. The Kim group reported yields in the 10^{-7} range,[13-17] as well as a series of systematic observations, formulated as a set of MALDI "rules", which they concluded must exclude non-thermal models.[18] The non-thermal CPCD has since been shown to be fully consistent with these rules, so they are are not proof of thermal ionization.[19] This group also argued for a thermal autoprotolysis mechanism, without necessarily invoking a polar fluid.[20]

Yields in the 10^{-9} to 10^{-6} range were also reported in ref. [21], supporting the Kim results. This group also proposed a purely thermal ionization mechanism, and recently presented a detailed implementation of the polar fluid model.[22] The central aspect of the PFM, solvent stabilization of ion pairs, was calculated using dielectric response theory to estimate the matrix fluid dielectric constant, the key factor in reducing the energetics of ion pair formation. If reaction equilibrium is assumed, the expected ion concentration is then easily determined, at a given temperature. Since the MALDI plume cools as it expands, the ion yield might be expected to reflect the final temperature, but it was argued that the neutralization reaction rate must be negligible, so that the yield rather reflects the peak temperature reached during the ablation event. With this framework and assumptions, and taking the matrix 2,5 dihydroxybenzoic acid (DHB) as an example, yields were calculated which were reasonably consistent with the newest measurements, but lower than older ones.

In the present work, matrix fluid ion stabilization, reaction equilibrium and recombination kinetics are reexamined theoretically. The results show that the PFM must play a very minor role in ultraviolet MALDI ion generation.

Methods

Ab initio molecular polarizability calculations were performed with the TDHFX package in the GAMESS suite.[23, 24] The molecular geometries were fully optimized at the RHF 6-31G(d,p) ++ level before the polarizability calculations.

Results and Discussion

Ion Formation Energetics and Dielectric Screening

Creation of ion pairs from two matrix neutrals is a very energetic process in the gas phase. Radical cation/anion pair generation requires 720 kJ/mol for DHB while autoprotolysis to a protonated/deprotonated pair requires less, about 502 kJ/mol.[25]

As noted in ref. 22 the equilibrium yield of positive matrix ions from the reaction $2M \rightarrow M^+ + M^-$ is below the recently reported yields unless the free energy of reaction can be reduced to 100-200 kJ/mol. Most, but not all, of the energy required for ion pair formation is in electrostatic charge separation. The electrostatic energy *E* is reduced if separation takes place in a medium with a relative permittivity, ε_R, greater than 1:

$$E(electrostatic) = \frac{E_0}{\epsilon_R \epsilon_0} \quad (1)$$

Where *Eo* is the energy in vacuum, and ε_0 is the permittivity of free space. Hereafter we refer to ε_R as the dielectric constant of the material.

Low Temperature Dielectric Constant

Because of the reduction of reaction free energy it brings, a high dielectric constant of the matrix fluid is a critical part of the PFM. Being solid at room temperature and in many cases decomposing at high temperature,[26] the dielectric properties of matrix fluids at MALDI-relevant temperatures and pressures are not easily measured. One approach is to use the theory of ideal dielectrics, in particular the Clausius-Mossotti and Kirkwood-Fröhlich relationships.[22]

The Clausius-Mossotti equation relates the molecular polarizability to the "optical" dielectric constant. The permittivity at high frequency, *ε(opt)*, is determined only by the response of the fastest part of the system, the electron cloud:

$$\epsilon(opt) = \frac{(2K+1)}{(1-K)} \qquad K = 4\pi/(3\alpha\rho) \quad (2)$$

The material density is denoted by ρ and the polarizability by α. For nonmagnetic materials, the optical dielectric constant is also directly related to the index of refraction:

$$\epsilon(opt) = \eta^2 \quad (3)$$

The Kirkwood-Fröhlich equation connects the high frequency dielectric constant and the molecular diplole moment, μ, to the static dielectric constant ε. Both fast and slow responses are included. (The orientation factor, g, which normally multiplies μ on the left hand side, is here taken to be unity, since MALDI is a high temperature process):

$$\mu^2 = \frac{9kT(\epsilon - \epsilon(opt))(2\epsilon + \epsilon(opt))}{4\pi\epsilon(\epsilon(opt)+2)^2} \quad (4)$$

Where k is the Boltzmann constant and T the absolute temperature. Polarizabilities are not yet experimentally known for MALDI matrixes, instead one may try to calculate them with ab initio theory, as in Ref. 22. A sufficiently high frequency must be specified such that only electronic polarization occurs. The polarizability of DHB calculated at several wavelengths (frequencies) using the GAMESS package is shown in Fig. 1.

Figure 1 here

While there is a small dependence of the polarizability on basis set, there is a large dependence on frequency, especially at short wavelengths, on the left side of Fig. 1. As is evident, essentially any polarizability larger than the zero frequency value can be obtained. The consequences of this for the dielectric constant at high and low frequency (static) are shown in Fig. 2.

Figure 2 here

The dielectric constants diverge at 4.3×10^{-23} cm^3. From the Kramers-Kronig transform, which connects the absorption spectrum with the frequency dependent dielectric constant, the cusp in Fig. 2 must correspond to an absorption band. Since the ab initio calculations were carried out for the ground state, no electronic transitions are included. The absorption band corresponds to the plasma frequency of the material. From Fig. 1, the corresponding notional absorption band center lies somewhere below 250 nm.

The absorption spectra of MALDI matrix materials are well known, and intense singlet-singlet absorptions begin in the near UV, typically well above 300 nm. The DHB S_1 electronic origin is at 357.69 nm in the gas phase, for example.[27] To correctly model DHB, Fig. 1 should exhibit peaks for every absorption band in the spectrum, not just a single one at the plasma frequency. Each of these will affect the dielectric constant across the spectrum, including at zero frequency. This is the basis for the widely used Sellmeier equations for refractive indexes, which include an explicit term for each absorption band.[28]

As is evident, ab initio calculations of molecular polarizability at optical frequencies are unsuitable for accurate estimation of static dielectric constants of MALDI matrix fluids. Not only is the method physically incomplete, but arbitrary and very large dielectric constants can be obtained by choice of frequency at which to calculate the polarizability.

Nevertheless, it is instructive to consider what the method predicts if the polarizability is calculated as far as possible from absorption bands, at zero nominal frequency. Some results are collected in Table 1. Measured static dielectric constants of some substances related to MALDI matrix materials at or near room temperature are: phenol 10, methyl salicylate 9, acetophenone 17, cinnamaldehyde 17.[29]

Table 1 here

The reason for the factor of two difference between the DHB static dielectric constants calculated using GAMESS and Gaussian is unknown. More remarkable are the high to extremely high values calculated for the other matrices. As tables of dielectric constants show, values of 30 are uncommon, while 75 or higher is quite rare. The calculated values do not seem reasonable, confirming that this procedure for estimating dielectric constants is insufficient for evaluating thermal ionization models.

High Temperature Dielectric Constant

The PFM requires both strong solvating ability and high temperature to achieve relevant ion yields. It is therefore necessary to estimate the dielectric constant of a putative matrix fluid at high temperatures, not just at room temperature.

At 1000 K, the Clausius-Mossotti and Kirkwood-Fröhlich equations predict $\varepsilon=5$ for DHB, assuming no change of density. In Ref. 22 the matrix fluid was taken to expand as a normal liquid with a thermal expansion coefficient typical of fluids near room temperature, with no phase change. Since all useful matrixes are volatile at relatively low temperatures[30] this approximation seems open to question.

Molecular dynamics suggests that a MALDI ablation event can often be described as a "phase explosion" in which the material undergoes rapid, inhomogeneous (frothy) conversion from solid to gas.[31] The material clearly expands more than if it remained a simple liquid. Before it cools significantly from the peak, simulations show the volume increases by at least a factor of two, depending on the depth of the ablated layer under consideration.[32-34] This reduces the predicted 1000 K dielectric constant of DHB to <2.2.

At least as important as these theoretical estimates are comparisons to real materials. In the pressure range predicted by molecular dynamics simulations of MALDI, a few MPa, the dielectric constant of water at 850 K is 1.01 (1 MPa) to 1.10 (10 MPa).[35] (P_c(water)=22 MPa). The low temperature dielectric constant of DHB fluid is certainly well below that of

water, so it appears extremely unlikely that it's dielectric constant under MALDI conditions is larger than 1.1.

Further, predicted peak MALDI temperatures and pressures exceed the critical point of many substances.[33] Compare benzene, 562 K, 4.9 MPa; benzoic acid, 752 K, 4.5 MPa; and phenol, 694 K, 6.1 MPa.[36] It is possible that DHB matrix fluid also becomes supercritical in a MALDI event. A common characteristic of supercritical fluids is a very low dielectric constant, and a consequent poor ability to solvate ions. The expected dielectric constant in that case would presumably lie even below the 1.1 value noted above for subcritical water.

Both theoretically and by comparison to experimental data, the conclusion seems unavoidable that the PFM is unable to explain MALDI ion yields for DHB because the reaction free energy remains much too high. Instead of the necessary 100-200 kJ/mol, the screened reaction energy will be at least 450-500 kJ/mol. The equilibrium ion yield is then in the 10^{-12} to 10^{-13} range, at 1000 K.

Ion Formation Reaction Rate

Evidence for lack of in equilibrium MALDI is routine, but this fact is seldom noted. For example, in the case of DHB matrix, M^+, MH^+ and Mm^+ (m=alkali cation) are often observed with similar intensities. Since the energetics of these ions vary by hundreds of kJ/mol, equilibrium is certainly not achieved, the intensities would otherwise differ by orders of magnitude. More systematic studies of this effect also exist. The weak dependence of analyte ion ratios on matrix, and hence proton transfer reaction free energy, were noted by Dashtiev et al[37] and Hillenkamp et al[38]. The data differed from equilibrium predictions by several orders of magnitude. Shortly thereafter, it was found that the data are consistent with the CPCD model, which predicted a kinetic limit for the ratios.[6, 39] In this section, we explore the kinetic limitations of the thermal PFM model.

Although there is strong reason to doubt that a matrix fluid could have a high solvating power under MALDI conditions, consider the case that it is as predicted in Ref. [22]. The reaction free energy might then be reduced to as low as 150 kJ/mol, during the high density, low temperature period of the ablation event. The *equilibrium* ion yield at the peak temperature might then reach the range of some experiments, see Fig. 2 Ref. [22]. However, equilibrium is only achieved when forward and reverse rates become equal, and MALDI is a fairly rapid event, so it is important to consider the kinetics of ion formation. Specifically, we wish to determine the integrated yield of the autoprotolysis ion formation reaction during the MALDI event:

$$2M \rightarrow MH^+ + (M\text{-}H)^-$$

Where M is a matrix molecule.

The forward rate was given by a collisional (transition state) reaction model, as used in Ref. 22 for the gas phase plume. (There it was used only to model recombination in the plume,

not for the matrix fluid, in which equilibrium was assumed at all times.):

$$k_{forward} = A\,\mathrm{e}^{-E/(kT)} \tag{5}$$

Where the prefactor *A* depends on density and temperature. The activation energy *E* is taken to the be the reaction free energy, ΔG.

In tandem with the expression for reaction equilibrium:

$$K = \mathrm{e}^{-\Delta G/(RT)} \tag{6}$$

the fundamental paradox of all thermal MALDI models slowly becomes apparent. Both yield and rate drop as ΔG/(RT) increases. Thermal equilibrium yields in the seemingly feasible 10^{-7} to 10^{-9} range[22] necessarily imply that the ion formation rate is too low to approach equilibrium on the necessary time scale of a few nanoseconds. Thermal models are, *in principle*, not just in detail, incapable of accounting for MALDI ion formation, unless *both* yield and temperature are much higher than in Ref. 22.

This is illustrated in Fig. 3. Although the CPCD model can easily be modified for this task, simulations were performed using only the assumptions, parameters and reaction models of Ref. 22. This included thermal expansion, heat capacity, plume gas expansion, and modulation of the reaction free energy by expansion. No recombination or ion loss was included. Even if the reaction free energy is assumed to go as low as 100 kJ/mol (before expansion), and the sample does not vaporize, and there are no ion losses, the integrated ion production remains well below the lowest experimental ranges. Ion formation was numerically integrated to a time of 25 ns after the peak of the laser pulse, which substantially exceeds the time at maximum temperature in a real MALDI event. Two sets of simulations were carried out, one assuming no change of phase from solid to vapor until after maximum ion formation, and one assuming that the sample vaporizes completely at 450 K.[30] In all cases, the formation rates are too low to reach or even approach equilibrium on the MALDI time scale.

In the much more realistic case that the sample does indeed vaporize at a temperature in the vicinity of its sublimation temperature, the yields are even lower, since the sample expands faster. The yield even drops slightly at higher fluence because the phase change occurs earlier in the ablation event.

Figure 3 here

Ion Recombination Rate

In Ref. 22 it was suggested that homogeneous ion recombination reaction rates at the concentrations predicted in the MALDI plume would be too low to affect the observed yield.

However, the homogeneous model is not correct for a proton transfer ionization mechanism. Cations and anions are not formed at uncorrelated locations, but rather as fully correlated geminal pairs. Particularly at low ion concentration, this results in different recombination kinetics than in the homogeneous case.

Geminate recombination is a key concept in studies of phenomena such as excited state proton transfer (ESPT),[40] or reactions between defects in irradiated solids.[41] Within the Onsager or Debye radius, where the Coulomb energy is equal to or less than thermal energy, the geminate recombination rate is high. Outside it asymptotically approaches the diffusion limit.[40] Note that the low dielectric constant means that the Debye radius in matrix fluid will be large:

$$R_D = \frac{e^2}{kT\epsilon} \tag{7}$$

Where e is the electron charge, and k the Boltzmann constant. A Debye-Smoluchowski equation including the electrostatic force between the ion pair needs to be solved for the survival probability of the ions after formation. The kinetic equation takes into account the relative diffusion constant of the ions with respect to each other. Certainly a matrix fluid will not allow protons to diffuse nearly as fast as in low molecular weight, highly networked protic solvents like water. The large R_D and slow diffusion mean that a new ion pair will remain in near-contact for a long time, increasing the recombination rate and reducing the survival probability.

In the "black sphere" model, geminate recombination is assumed to take place immediately and irreversibly at an intermolecular radius *Ro*. Obviously, if ions are initially formed at or within this radius, none can escape. If they are formed at a larger radius (but possibly still within the Debye radius), some will escape by diffusion. The larger the formation radius, *R*, the larger the escaping fraction. The total fraction of isolated geminate pairs which separate and survive, *S*, integrated from the time of formation to infinity, at temperature *T* is:[41]

$$S(R, T, t=\infty) = \left(\frac{e^{R_D/R_o} - e^{R_D/R}}{e^{R_D/R_o} - 1} \right) e^{(-R_D/R)} \tag{8}$$

The quotient of differences in the left bracket varies from 0 to 1, as *R* increases. The exponent in the rightmost factor includes the Coulomb energy of the ion pair at the formation distance. The Coulomb energy is the largest part of the reaction free energy, but not all of it, so we can take to be slightly less than ΔG. The exponential factor dominates the left bracket, at all *R* not extremely close to *Ro*.

To extend Fig. 3 to include geminate recombination, the curves should be convolved with *S(R,T, t)* for some *R* distribution. Since the infinite time survival fraction *S(R,T,t=∞)* is larger than all *S(R,T,t<∞)* we *overestimate* the total ion formation rate if we multiply the curves in

Fig. 3 by $S_{max}=S(R=large,T=T_{max},t=\infty)$. At 1000 K, and ΔG=100 kJ/mol, S_{max}= 6x10^{-6}.

Even without ion recombination, the thermal formation rates in MALDI are too low to be compatible with experimental yields. With geminate recombination, and assuming favorable parameters, the rates drop by at least 6 orders of magnitude. The corresponding yields during the few nanoseconds of a MALDI event are obviously similary impacted.

Conclusions

Three aspects of the polar fluid model of MALDI ionization were reexamined: reduction by dielectric screening of the energy required for ion formation, thermal ion equilibrium vs formation rates, and ion recombination rates.

The ab initio Clausius-Mossotti/Kirkwood-Fröhlich approach to estimation of matrix fluid dielectric constants is physically incomplete in neglecting the absorption spectrum, and makes arbitrary and implausible predictions. Even applying it at low frequency, where errors should be minimized, the upper estimate for the dielectric constant of a DHB fluid at high temperature is about 2. This is too low to explain MALDI yields, even in an equilibrium model.

Probably much more relevant, however, is comparison to real materials. Even subcritical water at temperatures and pressures below those in a MALDI event has a dielectric constant below 1.1. Comparison with related substances also suggest it is likely that DHB fluid would be supercritical, reducing the dielectric constant further. Given such dielectric constants, and at MALDI peak temperatures, the equilibrium ion yield is several orders below the lowest experimental values, in the range of 10^{-12} to 10^{-13}.

The fundamental yield/rate paradox of thermal models shows that equilibrium on the MALDI time scale is not achievable. Using rate theory previously applied only to the reverse, recombination, reaction in the plume, the ion yield during the short MALDI event is found to be far below the thermal equilibrium values. Even at a very low reaction energy (100 kJ/mol), with no recombination, no phase change/drop in density and integrating over an unrealistically long time at high temperature, the yield is in the range of 10^{-11}. Including the phase change reduces the expected yield to 10^{-16}, again at 100 kJ/mol reaction energy. At a ΔG of 450-500 kJ/mol, consistent with probable values of the dielectric constant, the predicted yield is in the range of 10^{-25} to 10^{-26} instead of 10^{-12} to 10^{-13} at equilibrium.

Finally, geminate recombination strongly limits possible ion yields in a proton transfer thermal ionization model. Since protonated/deprotonated ion pairs must be formed in close proximity, and proton mobility in a matrix fluid must be low, most ions recombine before they escape by diffusion. Ion formation rates, and therefore yields on the MALDI time scale, fall by at least another factor of 10^6.

When all factors are considered together, the most probable thermal ion yield in the PFM model is less than 10^{-30}. In contrast to the conclusions of refs. 22 and 20, no remotely

significant role for thermal ionization under typical MALDI conditions seems to be possible.

These results are also of interest for models of so-called ambient ionization mechanisms. If thermal mechansims are incapable of predicting ion yields in the high-temperature MALDI case, they would seem to be definitively excluded for ambient ionization. In turn, this means that some form of non-thermal local energy concentration mechanism must take place. The lowest energy degree of freedom not populated at ambient temperature is that of electronic excitations. This degree of freedom also has the right magnitude for storing and releasing sufficient energy for ionization, a few electron volts. Models related to the CPCD might therefore be the most promising for exploring mechanisms of ambient ionization.

References

1. Karas, M., Glückmann, M., Schäfer, J.: Ionization in MALDI: singly charged molecular ions are the lucky survivors. *J. Mass Spectrom.,* **35**, 1-12 (2000)
2. Jaskolla, T. W., Karas, M.: Compelling Evidence for Lucky Survivor and Gas Phase Protonation: The Unified MALDI Analyte Protonation Mechanism. *J. Am. Soc. Mass Spectrom.,* **22**, 976-988 (2011)
3. Karas, M., Krueger, R.: Ion Formation in MALDI: the cluster ionization mechanism. *Chem. Rev.,* **103**, 427-439 (2003)
4. Knochenmuss, R.: A Quantitative Model of Ultraviolet Matrix-assisted Laser Desorption and Ionization. *J. Mass Spectrom.,* **37**, 867-877 (2002)
5. Knochenmuss, R.: A Quantitative Model of UV-MALDI Including Analyte Ion Generation. *Anal. Chem.,* **75**, 2199 (2003)
6. Knochenmuss, R.: A bipolar rate equation model of MALDI primary and secondary ionization processes, with application to positive/negative analyte ion rations and suppression effects. *Int. J. Mass Spectrom.,* **285**, 105-113 (2009)
7. Knochenmuss, R.: MALDI mechanisms: wavelength and matrix dependence of the coupled photophysical and chemical dynamics model. *The Analyst,* **139**, 147-156 (2014)
8. Allwood, D. A., Dyer, P. E., Dreyfus, R. W.: Ionization Modeling of Matrix Molecules in Ultraviolet Matrix-Assisted Laser Desorption/Ionization. *Rapid Commun. Mass Spectrom.,* **11**, 499-503 (1997)
9. Allwood, D. A., Dyer, P. E., Dreyfus, R. W., Perera, I. K.: Plasma Modeling of Matrix-Assisted UV Laser-Desorption/Ionization (MALDI). *Appl. Surf. Sci.,* **110**, 616-620 (1997)
10. Niu, S., Zhang, W., Chait, B. T.: Direct Comparison of Infrared and Ultraviolet Wavelength Matrix-Assisted Laser Desorption/Ionization Mass Spectrometry of Proteins. *J. Am. Soc. Mass Spectrom.,* **9**, 1-7 (1998)
11. Chen, X., Carroll, J. A., Beavis, R. C.: Near-Ultraviolet-Induced Matrix-Assisted Laser Desorption/Ionization as a Function of Wavelength. *J. Am. Soc. Mass Spectrom.,* **9**, 885-891 (1998)
12. Zenobi, R., Knochenmuss, R.: Ion Formation in MALDI Mass Spectrometry. *Mass Spectrom. Rev.,* **17**, 337 (1998)
13. Bae, Y. J., Moon, J. H., Kim, M. S.: Expansion Cooling in the Matrix Plume is Under-Recognized in MALDI Mass Spectrometry. *J. Am. Soc. Mass Spectrom.,* **22**, 1070-1078 (2011)
14. Bae, Y. J., Park, K. M., Kim, M. S.: Reproducibility of Temperature-Selected Mass Spectra in Mastrix-Assisted Laser Desorption Ionization of Peptides. *Anal. Chem.,* **84**, 7107-7111 (2012)
15. Bae, Y. J., Shin, Y. S., Moon, J. H., Kim, M. S.: Degree of Ionization in MALDI of Peptides: Thermal Explanation for the Gas-Phase Ion Formation. *J. Am. Soc. Mass Spectrom.,* **23**, 1326-1335 (2012)
16. Moon, J. H., Shin, Y. S., Bae, Y. J., Kim, M. S.: Ion Yields for Some Salts in MALDI: Mechanism for the Gas-Phase Ion Formation from Preformed Ions. *J. Am. Soc. Mass Spectrom.,* **23**, 162-170 (2011)
17. Moon, J. H., Yoon, S. H., Kim, M. S.: Temperature of Peptide Ions Generated by Matrix-

Assisted Laser Desorption Ionization and Their Dissociation Kinetic Parameters. *J. Phys. Chem. B,* **113**, 2071-2076 (2009)
18. Ahn, S. H., Park, K. M., Bae, Y. J., Kim, M. S.: Quantitative reproducibility of mass spectra in matrix-assisted laser desorption ionization and unraveling of the mechanism for gas-phase peptide ion formation. *J. Mass Spectrom.,* **48**, 299-305 (2013)
19. Knochenmuss, R.: MALDI Ionization Mechanisms: the Coupled Photophysical and Chemical Dynamics Model Correctly Predicts "Temperature"-Selected Spectra. *J. Mass Spectrom.,* **48**, 998-1004 (2013)
20. Bae, Y. J., Choe, J. C., Moon, J. H., Kim, M. S.: Why do the Abundances of Ions Generated by MALDI Look Thermally Determined? *J. Am. Soc. Mass Spectrom.,* **24**, 1807-1815 (2013)
21. Tsai, M.-T., Lee, S., Lu, I.-C., Chu, K. Y., Liang, C.-W., Lee, C. H., Lee, Y. T., Ni, C.-K.: Ion-to-neutral ratio of 2,5 dihydroxybenzoic acid in matrix-assisted laser desorption/ionization. *Rapid Comm. Mass Spectrom.,* **27**, 955-963 (2013)
22. Chu, K. Y., Lee, S., Tsai, M.-T., Lu, I.-C., Dyakov, Y. A., Lai, Y. H., Lee, Y.-T., Ni, C.-K.: Thermal Proton Transfer Reactions in Ultraviolet Matrix-Assisted Laser Desorption/Ionization. *J. Am. Soc. Mass Spectrom.,* 310-318 (2014)
23. Gordon, M. S., Schmidt, M. W.: Advances in electronic structure theory: GAMESS a decade later. **Theory and Applications of Computational Chemistry, the first forty years**, Elsevier, Amsterdam, 1167-1189 (2005)
24. Schmidt, M. W., Baldridge, K. K., Boatz, J. A., Elbert, S. T., Gordon, M. S., Jensen, J. J., Koseki, S., Matsunaga, N., Nguyen, K. A., Su, S., Windus, T. L., Dupuis, M., Montgomery, J. A.: GAMESS. *J. Comput. Chem.,* **14**, 1347-1363 (1993)
25. Knochenmuss, R.: Ion formation mechanisms in UV-MALDI. *The Analyst,* **131**, 966-986 (2006)
26. Tarzi, O. I., Nonami, H., Erra-Balsells, R.: The effect of temperature on the stability of compounds used as UV-MALDI-MS matrix: 2,5 DHB, 2,4,6 THAP, CHCA, 35, dimethoxy-4-hydroxycinnamic acid, nor-harmane and harmane. *J. Mass Spectrom.,* **44**, 260-277 (2009)
27. Karbach, V., Knochenmuss, R.: Do Single Matrix Molecules Generate Primary Ions in Ultraviolet Matrix-Assisted Laser Desorption/Ionization? *Rapid Commun. Mass Spectrom.,* **12**, 968-974 (1998)
28. Sellmeier, W.: Zur Erklärung der abnormen Farbenfolge im Spectrum einiger Substanzen. *Annalen der Physk und Chemie,* **219**, 272-282 (1871)
29. Maryott, A. A., Smith, E. R.: Table of Dielectric Constants of Pure Liquids. *National Bureau of Standards Circular 514,* (1951)
30. Stevenson, E., Breuker, K., Zenobi, R.: Internal energies of analyte ions generated from different matrix-assisted desorption/ionization matrices. *J. Mass Spectrom.,* **35**, 1035-1041 (2000)
31. Zhigilei, L. V., Garrison, B. J.: Microscopic mechanism of laser ablation of organic solids in the thermal stress confinement irradiation regime. *J. Appl. Phys.,* **88**, 1 - 18 (2000)
32. Knochenmuss, R., Zhigilei, L. V.: A molecular dynamics model of UV-MALDI including ionization processes. *J. Phys. Chem. B,* **109**, 22947-229957 (2005)
33. Knochenmuss, R., Zhigilei, L. V.: Molecular dynamics simulations of MALDI: laser fluence and pulse width dependence of plume characteristics and consequences for matrix and

analyte ionization. *J. Mass Spectrom.,* **45**, 333-346 (2010)
34. Knochenmuss, R., Zhigilei, L. V.: What Determines MALDI Ion Yields? A Molecular Dynamics Study of Ion Loss Mechanisms. *Anal. Bioanal. Chem.,* **402**, 2511-2519 (2012)
35. Uematsu, M., Franck, E. U.: Static Dielectric Constant of Water and Steam. *J. Phys. Chem. Ref. Data,* **9**, 1291-1306 (1980)
36. NIST Chemistry WebBook, NIST Standard Reference Database Number 69. National Institute of Standards and Technology, Gaithersburg MD,
37. Dashtiev, M., Wäfler, E., Röhling, U., Gorshkov, M., Hillenkamp, F., Zenobi, R.: Positive and negative analyte ion yield in matrix-assisted laser desorption/ionization. *Int. J. Mass Spectrom.,* **268**, 122-130 (2007)
38. Hillenkamp, F., Wäfler, E., Jecklin, M. C., Zenobi, R.: Positive and negative analyte ion yield in MALDI revisited. *Int. J. Mass Spectrom.,* **285**, 114-119 (2008)
39. Knochenmuss, R.: Positive/negative ion ratios and in-plume reaction equilibria in MALDI. *Int. J. Mass Spectrom.,* **273**, 84-86 (2008)
40. Agmon, N.: Elementary Steps in Excited-State Proton Transfer. *J. Phys. Chem. A,* **109**, 13-35 (2005)
41. Kotomin, E., Kuzovkov, V.: Phenomenological kinetics of Frenkel defect recombination and accumulation in ionic solids. *Rep. Prog. Phys.,* **55**, 2079-2188 (1992)
42. Jaskolla, T. W., Lehmann, W. D., Karas, M.: 4-Chloro-a-cyanocinnamic acid is an advanced, rationally designed MALDI matrix. *Proc. Nat. Acad. Sci. U.S.A.,* **105**, 12200-12205 (2008)

Figures

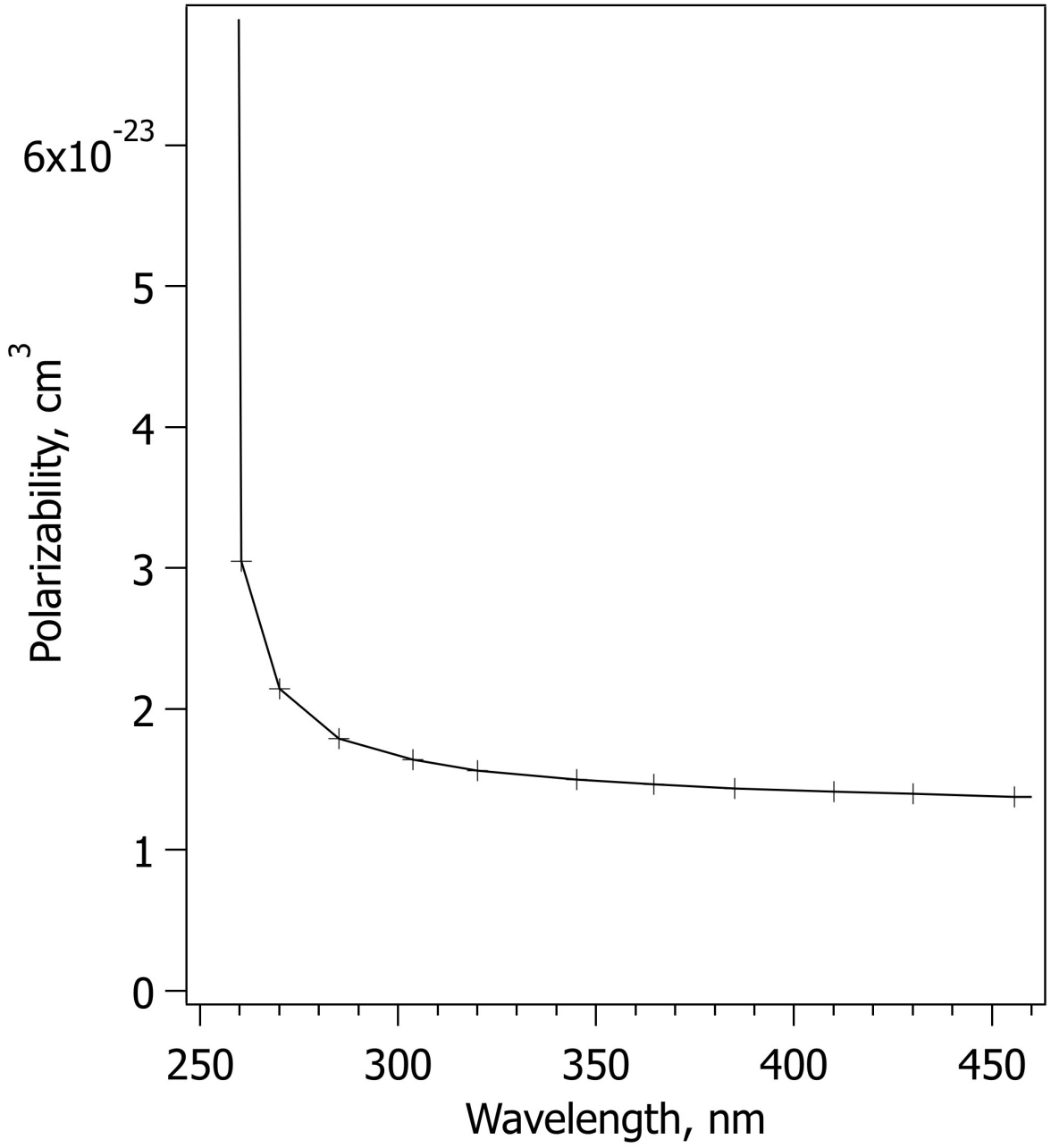

Figure 1. Ab initio DHB polarizability, at the RHF 6-31G(d,p)++ level, as a function of the wavelength of the applied field. No electronic absorptions have been taken into account.

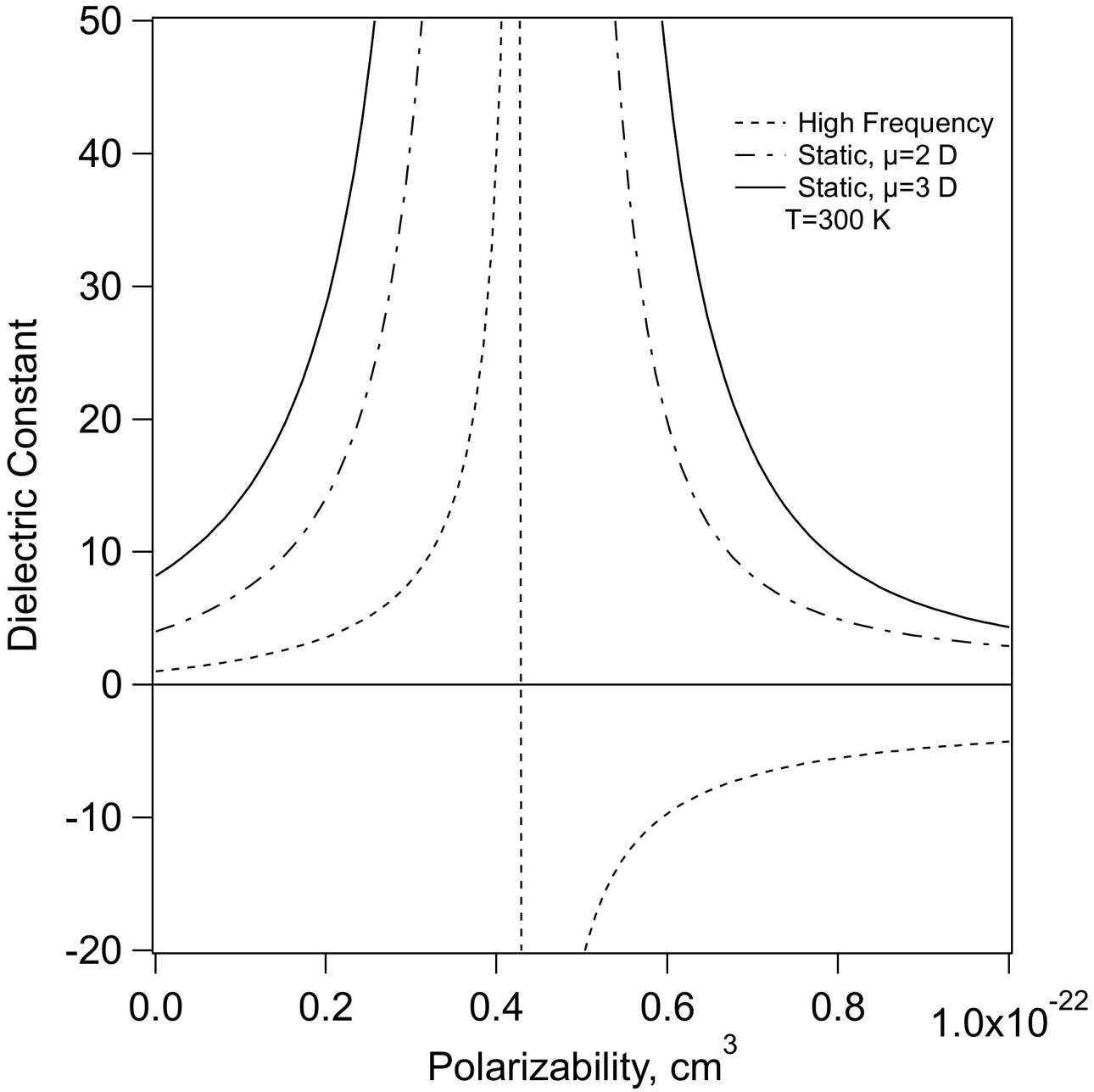

Figure 2. High frequency and static dielectic constants of DHB as a function of molecular polarizability and dipole moment, as calculated using the Clausius-Mossotti and Kirkwood-Fröhlich equations. The density was as in ref. 22.

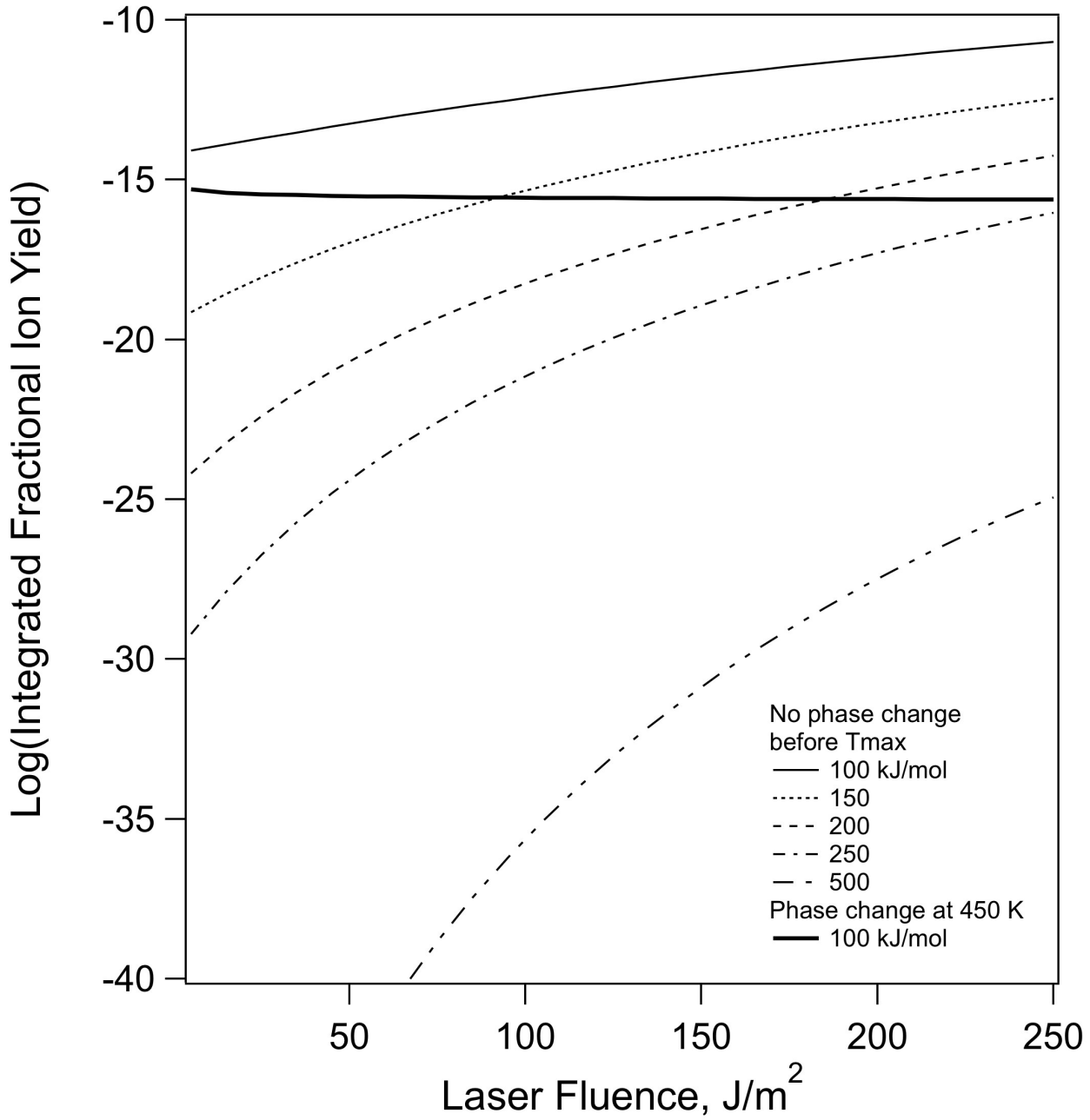

Fig. 3. Thermal ion yield calculated by integration of the proton transfer ion formation rate equation, for DHB. The laser pulse was 5 ns FWHM, 355 nm. All matrix properties were as in Ref. 22. The recombination rate was taken to be zero. Including geminate recombination, the curves must be divided by a factor $1/S_{max} >= 10^6$. See the text for further details.

Table 1. Dielectric constants for some MALDI matrix molecules calculated using the Clausius-Mossotti and Kirkwood-Fröhlich equations. The polarizabilities and dipole moments were calculated using the 6-31G(d,p)++ basis in GAMESS. The density was held constant as in Fig. 1, the temperature was 300 K. CHCA=cyanohydroxycinnamic acid, ClCCA= 4-chloro-cyanocinnamic acid,[42] THAP=trihydroxyacetophenone.

matrix	dipole, Debye	α, 10^{-23} cm^3	ε(opt)	ε(static)
DHB	2.17	1.28	2.6	11
DHB*	2.8	1.84	3.3	22
CHCA	3.55	2.63	5.8	76
ClCCA	2.87	2.03	3.7	27
THAP	3.84	1.45	2.5	30

* From Ref. 22, Gaussian09, MP2/6-31G(d)+, frequency unknown.